Electronic Supplementary Material (ESI) for New Journal of Chemistry.

Supporting Information

Counterion Controlled Synthesis of Multifunctional Iron Cobalt Mixed Oxides Laminar Superstructures

Nureena Kanwal, [a] Bilal Akram, [b] Chaudry Sajed Saraj, [c,d] Khalil Ahmad, [a] Shamraiz Hussain Talib[e] and Hafiz Muhammad Asif [f]

Experimental methodology

Synthesis of FeCo mixed oxide laminar superstructures (FCLS)

In a typical synthesis, a solution was prepared by adding 1ml of oleic acid (OA) and 0.05g of octadecyl amine (ODA) into 3ml of n-hexane. Another solution was prepared by dissolving 1.41g of cobalt sulphate and 1.39g of iron sulphate in 7 ml of distilled water. Both solutions (solution of OA+ODA and of salts) were mixed and stirred for 15min. The resulting solution was being kept in the oven at 80^0C for 12 hours. The product was separated and purified by centrifugation using ethanol and cyclohexane. The obtained mixed oxide laminar superstructures were dried in an oven and subjected for characterization and catalysis.

Similar synthetic strategy with different metals precursors was used to obtain different nanostructures. For instance, use of acetate precursor of both iron and cobalt leads to nanoclusters and nanosheets were obtained using chloride precursors of both the metals.

Characterization of Materials.

The structural characterizations of prepared samples were done by using transmission electron microscopy (TEM) (Hitachi, H-800; operated at 200kV), and X-ray diffraction (Rigaku, Smartlab; operated at 40kV and 200mA, Cu Kα source). Energy Dispersive X-ray spectroscopy coupled with electron microscopy (EDX) was employed to determine the elemental composition of the catalyst. The surface functional groups and successful preparation of target material was determined by applying Fourier transform infrared (FTIR) analysis using FTIR spectrometer (FTIR-2000, Bruker). The photo luminance (PL) and diffused reflectance spectra were recorded on a UV–Vis spectrophotometer (Shimadzu-1601). Thermogravimetric analysis (TGA) was performed with Mettler Toledo TGA/SDTA851e at a heating rate of 10 °C min^{-1} from room temperature to 700 °C under air flow. Brunauer-Emmett-Teller (BET) surface area was performed using a Quadrasorb SI-MP instrument. X-ray photoelectron spectroscopy (XPS) was performed on a scanning X-ray microprobe (Quantera SXM, ULVAC-PHI. INC) operated at 250 kV, 55 eV with monochromated Al Kα radiation.

Photocatalytic activity of FeCo mixed oxide nanostructures

Photocatalytic activity of FCLS and FCNPs was investigated using one of the most common textile dyes, methylene blue for degradation purpose. Catalytic performance was estimated by taking 50ml of known concentration of methylene blue (5ppm). 50mg of FeCo based nano catalyst was added to 50ml of dye solution which correspond to 1mg/ml of solution. The reaction was initiated by the addition of 1ml of hydrogen peroxide as oxidant into 50ml dye solution. To attain the adsorption and desorption equilibrium between catalyst and dye the solution was kept in the dark for 30 minutes. After dark treatment catalyst containing dye solution was kept on stirring under light irradiation. The progress of MB degradation was observed with successive time interval of 3 minutes and absorbance was measured at 663nm. Catalyst showed appreciable degradation activity for MB. While analysing the dye concentration syringe was used to take specific volume of solution to minimize catalyst injection. To analyse the recyclability and steadiness of catalyst, the catalyst was removed from dye solution after completion of experiment. Catalyst was separated using centrifuge machine, washed twice with water and twice with ethanol. Then oven dried and reused for stability test.

Electrochemical Measurements

Catalyst's ink of each sample was prepared by first ultrasonic dispersion of 5 mg of powder sample into 0.5 ml of water/ethanol solution (1:1, v/v) followed by the addition of 15 µl of 5% Nafion solution into mixture as adhesive and ultrasonication for 1 hour.

The working electrode (WE) was fabricated by deposition of 10 µl of prepared ink on a carbon-cloth electrode (area=1x1 cm^2) followed by drying at 25^oC temperature.

Electrochemical measurements were performed on BioLogic-VMP3 multichannel workstation with a three-electrode system, where a Pt-wire, a catalyst loaded carbon-cloth electrode, and a saturated calomel electrode (SCE) were used as counter, working and reference electrodes, respectively. An Aqueous solution of 1.0 M KOH were used as alkaline electrolytes for electrochemical tests. Linear sweep voltammetry (LSV) curves were measured by sweeping voltage in the range of -0.1 to 0.8 V vs SCE electrode with the scan rate of 10 mVs^{-1}. Expression $E_{RHE} = E_{SCE} + E^0_{SCE} + 0.0592 * pH$, where $E^0_{SCE} = 0.242\ V$, were used to convert V vs. SCE to V vs. reversible hydrogen electrode (RHE), all data were iR corrected. WE were first prestabilized in the electrolyte (1 MKOH) using 50 scans of cyclic voltammetry (CV) at 50 mV/s before performing LSV tests. Electrochemical impedance spectra (EIS) were recorded with the biasing of working electrode at and 0.5 V (OER) (vs SCE) and superimposing a small alternating voltage of 10 mV over the frequency range of $1x10^{-2}$ Hz to $1x10^6$ Hz. For double layer capacitance (C_{dl}) and electrochemical active surface area (ECSA), the small scan

CV were recorded in non-faradaic region from 0.1 to 0.26 V vs. SCE with different scan rates 10 mV/s, 20 mV/s, 40 mV/s, 60 mV/s, 80 mV/s, and 100 mV/s.

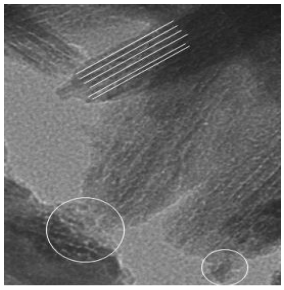

Figure S1. Zoom in TEM image clearly reveals the lamellar structure as indicated in schematic in the main MS. We 'have assumed that these laminar structures have been developed from the ultrafine nanoparticles. This proposed growth hypothesis has been evidenced by the existence of some aggregated nanoparticles as encircled in this TEM image. We assumed that these nanoparticles assembled into laminar structures and few particles remain unassembled in the product.

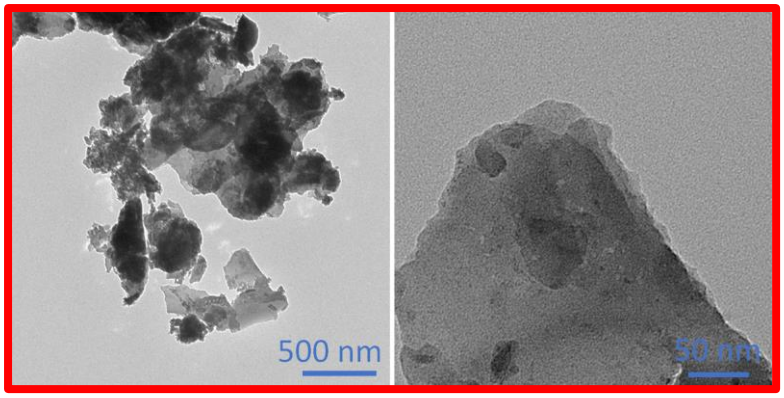

Figure S2. TEM image of the product obtained using chloride precursors of both metals

Scheme 1. The mechanistic details of the formation of mixed oxides is given below.

$FeSO_4 \quad H_2O \quad Fe^{2+} + SO_4^{2-}$

$CoSO_4 \xrightarrow{H_2O} Co^{2+} + SO_4^{2-}$

$RNH_2\ (ODA) \xrightarrow{\Delta} RNH_2^{+} + e^{-}$

$Fe^{2+} + Co^{2+} \xrightarrow{ODA,\ OA,\ Solvent} Fe\text{-}Co\text{-}O$

ODA can offer electrons as indicated above. So, the ODA solvent has some reducing power and the ability to attract electrons of metal ions determines the products. Since Fe and Co cannot attract electrons from ODA and thus mixed oxide is the product.

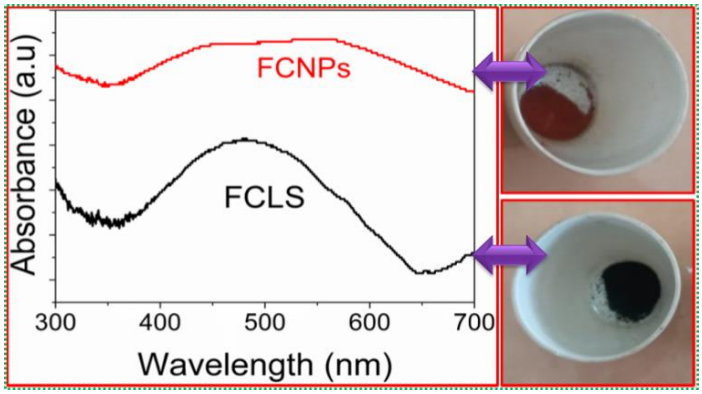

Figure S3. UV-Vis absorption spectrum and digital photographs of FCLS and FCNPs.

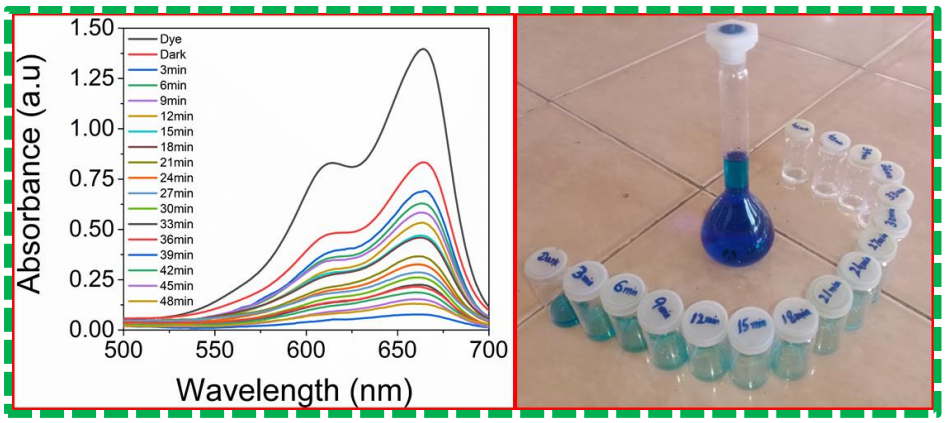

Figure S4. Photocatalytic performance of FCNPs: absorption spectrum of MB degradation and pictorial view of decolorization of MB

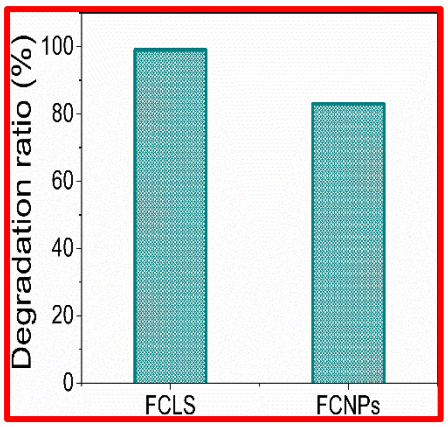

Figure S5. Degradation ratio after 30min irradiation over FCLS and FCNPs

FCLS		FCNPs	
BET summary		BET summary	
Slope =	25.051	Slope =	42.180
Intercept =	2.539e-01	Intercept =	1.502e+00
Correlation coefficient, r =	0.999968	Correlation coefficient, r =	0.999949
C constant=	99.660	C constant=	29.087
Surface Area =	137.623 m?g	Surface Area =	79.724 m?g

Figure S6. BET summary of both FCLS and FCNPs.

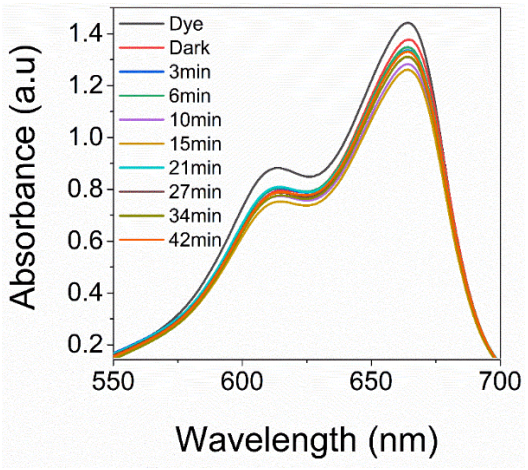

Figure S7. Photocatalytic degradation of MB using FCLS without H_2O_2

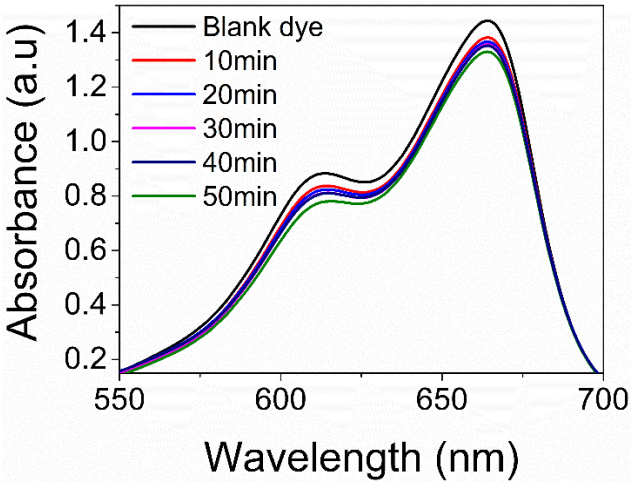

Figure S8. Photocatalytic degradation of MB using H_2O_2 without FCLS

Table S1. Different overpotential values for all the as-synthesized catalysts

Materials	η^{1} **(mV)**	η^{10} **(mV)**	η^{50} **(mV)**	η^{100} **(mV)**
CC	416	>800		
FCNPs	328	378	440	484
FCLS	283	330	380	412
IrO2	159	291	374	431

Table S2. The Tafel slopes and other electrochemical parameters for all the as-synthesized catalysts

Materials	η^{1} **(mV)**	η^{10} **(mV)**	**EIS** R_{ct} **(Ω)**	R_s **(Ω)**	C_{dl} **(mFcm^{-2})**	**Tafel slope (mVdec^{-1})**	J^{450} **(mAcm^{-2})**
CC	416	>800	43997	2.7	0.2	70	-
FCNPs	328	378	3.48	2.6	4.2	47	60
FCLS	283	330	2.49	2.19	30.6	45	175
IrO2	159	291					127

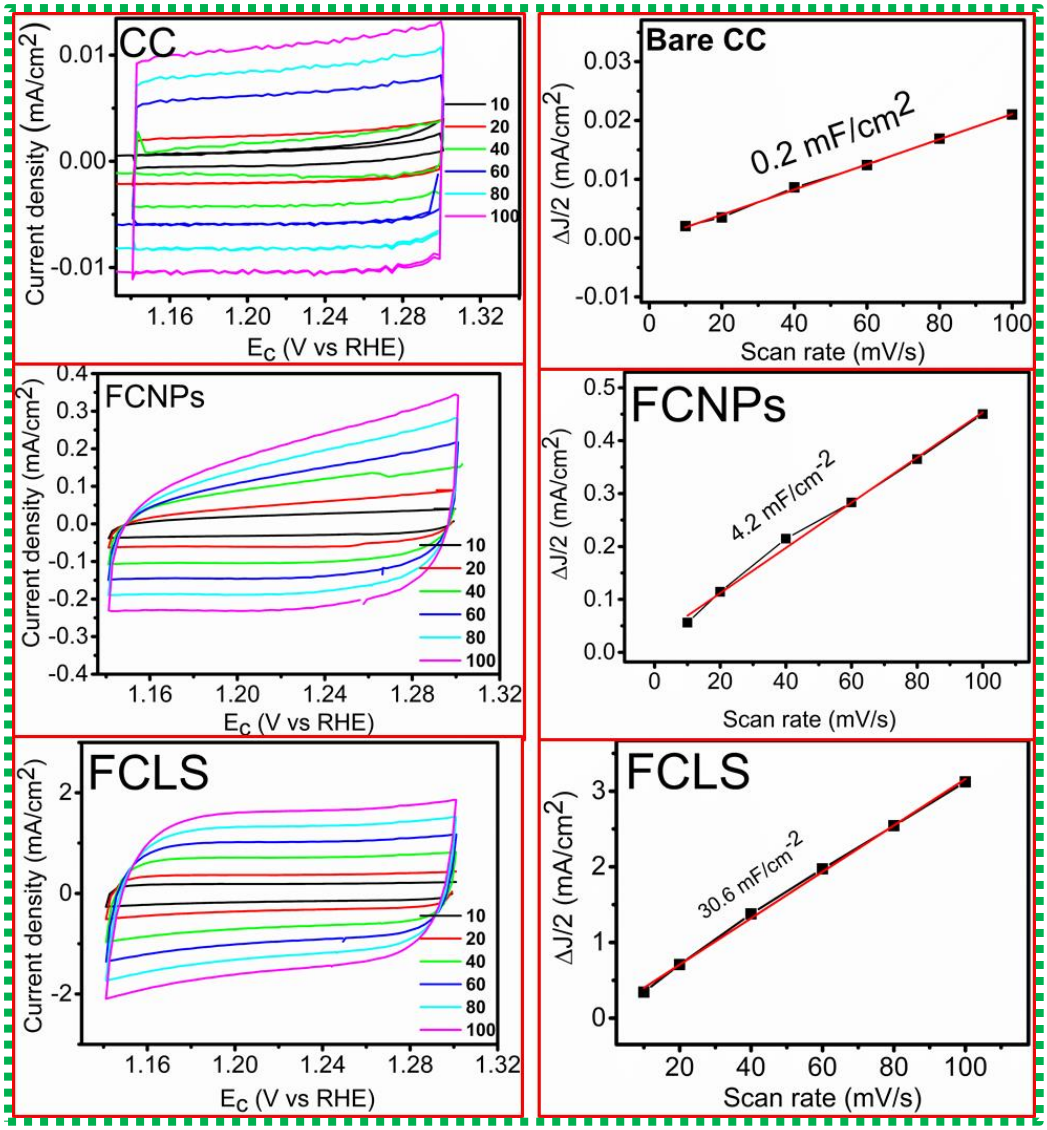

Figure S9. CV curves and Cdl of different samples

Table S3. The ECSA of various catalysts

Materials	Cdl ($mFcm^{-2}$)	C(CC) ($mFcm^{-2}$)	ECSA Cdl/C(NF) cm^2
CC	0.2	0.2	1
FCNPs	4.2	0.2	21
FCLS	30.6	0.2	153

Materials	preparation method	Electrolyte	Overpotential @10 $mAcm^{-2}$	Ref.
Sea-urchin structured Co-Fe-P	Chemical method	1 M KOH	370 mV	[1]
$CoFeO_x$	Electrodeposition	1 M NaOH	370 mV	[2]
Co/Fe oxide	Hydrothermal pathway	0.1M KOH	486 mV	[3]
$CoFe_2O_4$	Electrospinning and thermal treatment	0.1M KOH	370 mV	[4]
FeCo@NC	Electrospinning followed by pyrolysis	1M KOH	370 mV	[5]
CoFe-LDH/	Precipitation	1M KOH	331 mV	[6]
FeCo/CP	Co-precipitation followed by rapid pyrolysis	1M KOH	319 mV	[7]
Fe–Co_3O_4	Hydrothermal method	1M KOH	380 mV	[8]
Fe-Doped $NiCo_2O_4$	Hydrothermal method	1M KOH	350 mV	[9]
Fe-Doped CoOOH/G	Chemical synthesis	1M KOH	330 mV	[10]
Co_3O_4/$NiCo_2O_4$	Chemical synthesis	1M KOH	340 mV	[11]
FCLS	Solution phase synthesis	1M KOH	330 mV	*This work*
FCNPs	Solution phase synthesis	1M KOH	378 mV	*This work*

Table S4. Comparison of OER performance for various electrocatalysts in alkaline condition.

References:

1. A. Mendoza-Garcia, D. Su and S. Sun, *Nanoscale*, 2016, **8**, 3244-3247.
2. C. C. McCrory, S. Jung, J. C. Peters and T. F. Jaramillo, *J. Am. Chem. Soc.*, 2013, **135**, 16977-16987.
3. T. Grewe, X. Deng and H. Tüysüz, *Chem. Mater.*, 2014, **26**, 3162-3168.
4. M. Li, Y. Xiong, X. Liu, X. Bo, Y. Zhang, C. Han and L. Guo, *Nanoscale*, 2015, **7**, 8920-8930.
5. M. Li, T. Liu, X. Bo, M. Zhou and L. Guo, *Journal of Materials Chemistry A*, 2017, **5**, 5413-5425.
6. B. Zhang, X. Zheng, O. Voznyy, R. Comin, M. Bajdich, M. García-Melchor, L. Han, J. Xu, M. Liu and L. Zheng, *Science*, 2016, **352**, 333-337.
7. H. Zhang, J. Zheng, Y. Chao, K. Zhang and Z. Zhu, *New J. Chem.*, 2018, **42**, 7254-7261.
8. C. Xiao, X. Lu and C. Zhao, *Chem. Commun.*, 2014, **50**, 10122-10125.
9. K.-L. Yan, X. Shang, Z. Li, B. Dong, X. Li, W.-K. Gao, J.-Q. Chi, Y.-M. Chai and C.-G. Liu, *Appl. Surf. Sci.*, 2017, **416**, 371-378.

10. X. Han, C. Yu, S. Zhou, C. Zhao, H. Huang, J. Yang, Z. Liu, J. Zhao and J. Qiu, *Advanced Energy Materials*, 2017, **7**, 1602148.
11. H. Hu, B. Guan, B. Xia and X. W. Lou, *J. Am. Chem. Soc.*, 2015, **137**, 5590-5595.